Experimental report

30/01/2024

Proposal: **TEST-3244** **Council:** 4/2023

Title: Test of the Brillouin Neutron Scattering setup on IN8

Research area: Materials

This proposal is a new proposal

Main proposer: **Andrea PIOVANO**

Experimental team: Francesco SACCHETTI
Marco ZANATTA
Andrea ORECCHINI
Fabio BRUGNARA
Giacomo BALDI
Irene FESTI
Denis NABARI
Andrea PEGORETTI

Local contacts: Andrea PIOVANO

Samples: D2O, D2SO4
Ga, Sn, Al

Instrument	Requested days	Allocated days	From	To
IN8	7	12	19/06/2023	26/06/2023
			17/11/2023	22/11/2023

Abstract:

We intend to test the Brillouin neutron scattering on the new IN8 instrument, using known samples.

The aim of experiment TEST3244 is the validation and optimization of the Brillouin neutron scattering (BNS) setup for the three-axis thermal spectrometer IN8.
BNS requires a compromise between a low-exchanged wavevector Q, about 0.1-2 Å-1, a wide kinematic range, about tens of meV, and a high-energy resolution, to allow the discrimination of the Brillouin peaks from the elastic line. This means small-angle scattering using neutrons with high final energy and a high energy resolution (ΔE/E ~3%). These requirements can be achieved with a proper choice of the instrument setup. Moreover, to lower the air-scattering background, we installed a large-diameter cylindrical vacuum chamber. This is the primary background source for small-angle scattering.
To test this setup, we studied the collective dynamics of two molecular liquids: heavy water and deuterated sulfuric acid. Macroscopically and on enough long timescale, liquids are isotropic and do not support shear stresses. Consequently, their collective dynamics should be characterized by a longitudinal acoustic mode, and no transverse acoustic excitations. This holds at very low q, but approaching the microscopic domain, collective excitations show an unexpectedly rich pattern with two modes, e.g. Ref [1].

The first goal of this test experiment is to select and test the experimental configuration for BNS at IN8. We work at fixed final energy Ef because of the inverse geometry of the instrument. In the first attempt (June 2023), we exploit second-order harmonics both at the monochromator and the analyzer to increase the relative energy resolution without lowering Ef, thus keeping the dynamic range untouched. This approach is cumbersome because of the presence of unwanted harmonic contributions, arising from the monochromator, both at the monitor M1 and at the sample. In November, we tested what we claim as the final configuration: Si(311)-Cu(400). Here, no higher-order harmonic contributions arise from the monochromator: a monochromatic beam shines on the sample. The configuration was tested both with and without a PG filter to estimate the contribution of unwanted harmonics. The measure shows the absence of non-negligible contributions at the analyzer, supporting the no-PG filter configuration as the final one because of the higher efficiency.

In the following list, we present the 4 tested configurations. For the sake of conciseness, we will discuss only the final one.

1. Cu(400)-Cu(600) with a fixed final energy of 104.5 meV. Horizontal collimations are 20’/30’/20’/900’ (from the source to the detector). No vertical collimations are used. (June 2023)
2. Si(333)-Si(333) with a fixed final energy of 79.6 meV, with a graphite filter before the analyzer. Horizontal collimations are 20’/30’/20’/30’ (from the source to the detector). No vertical collimations are used. (June 2023)
3. Si(311)-Cu(400) with PG filter, tested with fixed final energy of 88.6 meV to exploit the filter. In this way, the first harmonic at the analyzer (energy Ef/4) is completely suppressed. However, also the second harmonic (Ef) is attenuated by a factor of 30-40 %. Horizontal collimations are set to 30’/30’/30’/900’ to have enough signal at the detector.
4. Si(311)-Cu(400) without PG filter tested at two final energies: k_f = 6 $Å^{-1}$ and kf = 5 $Å^{-1}$. The horizontal collimations are 20’/20’/30’/30’ (from the source to the detector), whereas no vertical collimations are used.

The final configuration: Si(311)-Cu(400)

To increase the resolution without affecting the dynamical range, in the first part of the test (June 2023) we exploited second or third-order harmonics at both the monochromator and the analyzer. However, the typical energies of neutrons make the situation cumbersome as unwanted harmonics are closer to the selected energy. In particular, we highlighted that, when using high-order harmonics at the monochromator, it is difficult to isolate the sample inelastic scattering signal of the chosen harmonic. Moreover, the monitor normalization shows problems since monitor counts are the sum of the chosen harmonic and the first one. For this reason, in this second try (November 2023), we decided to use a first harmonic at the monochromator.
We decided to test a configuration exploiting the Si(311) monochromator and the Cu(400) analyzer. Among the available monochromators, Si(311) has the lowest d-spacing, d = 1.63 Å. The Cu(400) analyzer roughly matches the monochromator d-spacing (d = 0.9 Å), thus guaranteeing the best resolution while preserving the flux. The expected energy resolution was calculated using Takin. Results show that the use of high-order harmonics at the monochromator does not significantly increase the resolution (about 5%), but adds unwanted components to the beam and decreases the flux. Measurements were done at fixed final wavevector k_f, namely k_f = 6 Å-1 (a) and k_f = 5 Å-1. Figure 1 shows a comparison of this configuration at the two E_f values.

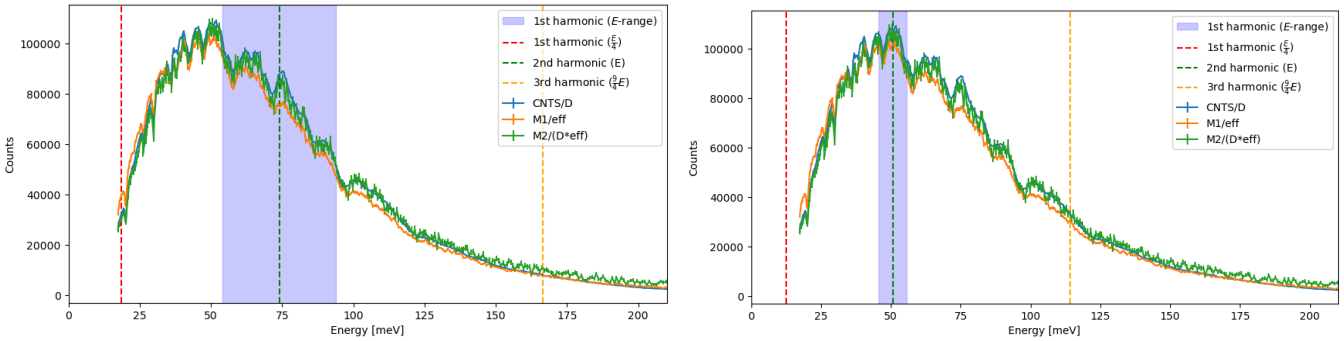

Figure 1. Si(311)-Cu(400) configuration with kf = 6 Å-1 (a) and kf = 5 Å-1 (b). The orange, green and blue lines are neutron flux measurements obtained with the first order of the Si(311) monochromator, respectively measured by the detector (CNTS), monitor 1 (M1) and monitor 2 (M2) (Vanadium sample, 2Θ=40o). To match the intensities, these are properly corrected by the monitor E-dependent efficiency and the Debye-Waller factor [2]. For our purposes, the orange line (monitor M1) corrected by the monitor efficiency gives a realistic estimation of the neutron flux. The coloured area represents the scanned energy ranges (here we assume Q = 1 Å-1, and a minimum scattering angle of 1°), whereas the dashed lines represent Ef. The range scanned by the monochromator using the second harmonic is not shown, as it lies above 500 meV and does not overlap with the thermal range.

1. Inelastic signal from the first harmonic

Figure 1 highlights that it is improbable that inelastic signals from the sample can enter the analyzer through unwanted harmonics because of the large distance with the scanned energy range. To test this, we exploited the PG filter, whose typical transmission is shown in Fig. 2. To test the presence of any inelastic signal rising from the second analyzer harmonic, we can use one of the two deeps in the transmission spectra of the PG filter.

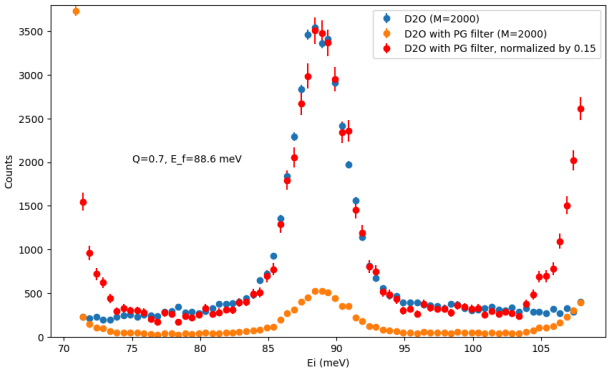

Figure 3. Comparison between the D2O spectra with (blue dots) and without PG filter (orange dots). Red dots show the peak normalised PG filtered spectrum (red dots), so the main effect of the filter is a strong reduction of the incident intensity.

Setting the final energy to 88.6 meV, we completely suppress any contribution from the first harmonic of the analyzer (22.15 meV deep in Fig. 2), and we attenuate the second harmonic intensity of 60 - 70% (note that this energy configuration E_f=88.6 meV is temporary, only to test the inelastic second harmonic contribution). Using D2O, we acquired two Q = 0.7 Å^{-1} spectra, with and without the graphite filter. Collimation was set as 30'/30'/30'/900' (from the source to the detector). Results are shown in Fig.3. Once normalized, the central part of the spectra are identical. This means that no high-order contamination impinges on the analyzer. Conversely, the PG filter increases the direct beam contributions which appear at the boundaries of the dynamic range. This may be caused by incoherent scattering on the filter.

2. Final configuration and energy resolution

The final horizontal collimation is 20'/20'/30'/30' (from the source to the detector), whereas no vertical collimations are used. We select two working final energies, depending on the exchanged wavevector Q. As can be seen from Fig. 4, below 0.3 Å^{-1} the dynamic range does not significantly increase by increasing the final energy E_f. Consequently, to properly explore this region, it is convenient to lower the final energy to increase the energy resolution.

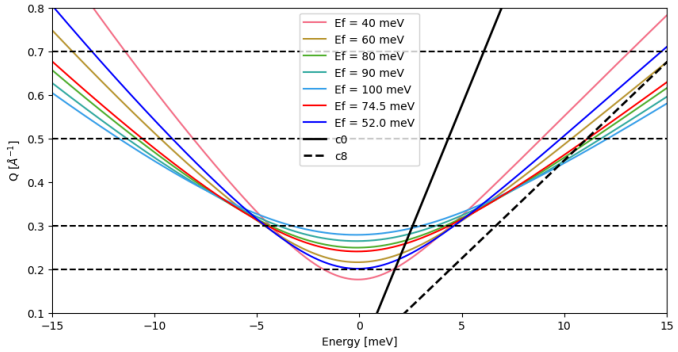

Figure 3. Dynamic range for different final energy configurations. The dynamic range curves are determined by assuming a minimum scattering angle of 2°.

Starting from the equation for the modulus of the exchanged momentum, we can write the width of the dynamic range Δω at a given exchanged wavevector Q as a function of the final energy Ef and the selected exchange wavevector:

$$\Delta\omega = \sqrt{\left(4E_f - \frac{Q^2}{c} - 4\cos^2(\theta_{min})E_f\right)^2 - 4\left(\frac{Q^4}{c^2} + 4E_f^2 - \frac{4E_fQ^2}{c} - 4\cos^2(\theta_{min})E_f^2\right)}$$

Starting from this equation and using Takin to calculate the E-resolution, we select two final wavevectors: kf = 6 Å^{-1} for Q ≥ 0.5 Å-1 and k_f = 5 Å-1 for Q = 0.3 Å-1.

Figure 5 shows the Vanadium spectrum measured at Q = 0.3 Å-1 on a Vanadium sample. As expected, the resolution is Gaussian and the FWHM (full width at half maximum) turns out to be 1.07 meV at k_f = 5 Å^{-1} and 2.10 meV at kf = 6 Å^{-1}.

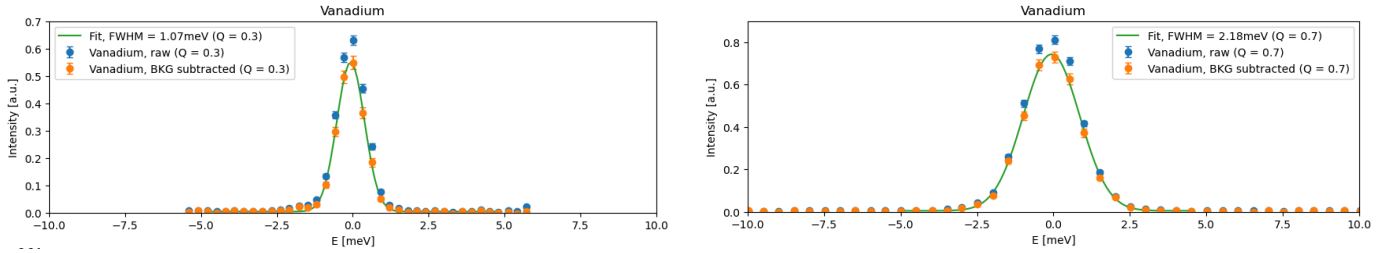

Figure 5. Vanadium spectra measured at Q = 0.3 Å-1 with kf = 6 Å-1 (left) and kf = 6 Å-1 (right). The red points are background subtracted data. The green line is the Gaussian fit to the data.

3. Background

Figure 6 shows the full absorber (Cadmium) and empty cell measurements. As can be seen, these do not show any anomaly and are roughly Q-independent.

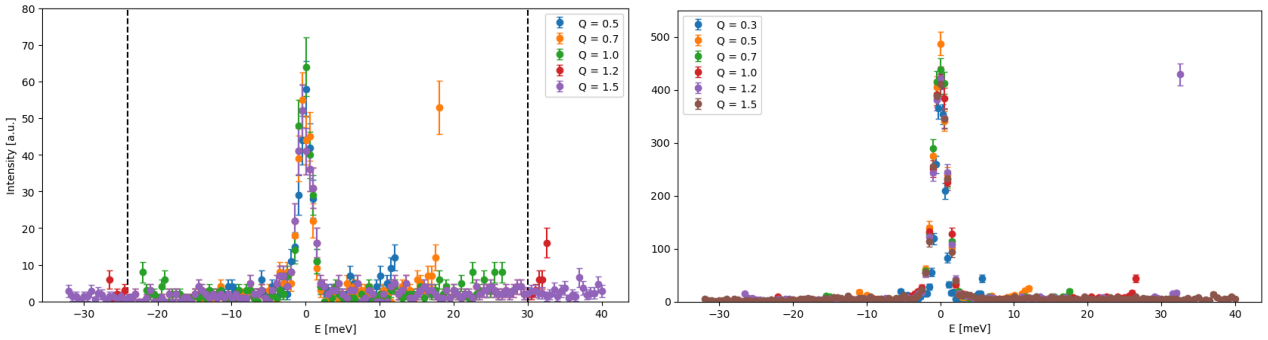

Figure 6. Empty cell (a) and Cadmium (b) measurements.

4. D_2O measurements

Finally, we show the D_2O data after the subtraction of the background. To highlight the inelastic contributions, the orange line shows the Vanadium spectrum, i.e. the resolution. The presence of an inelastic contribution is evident.

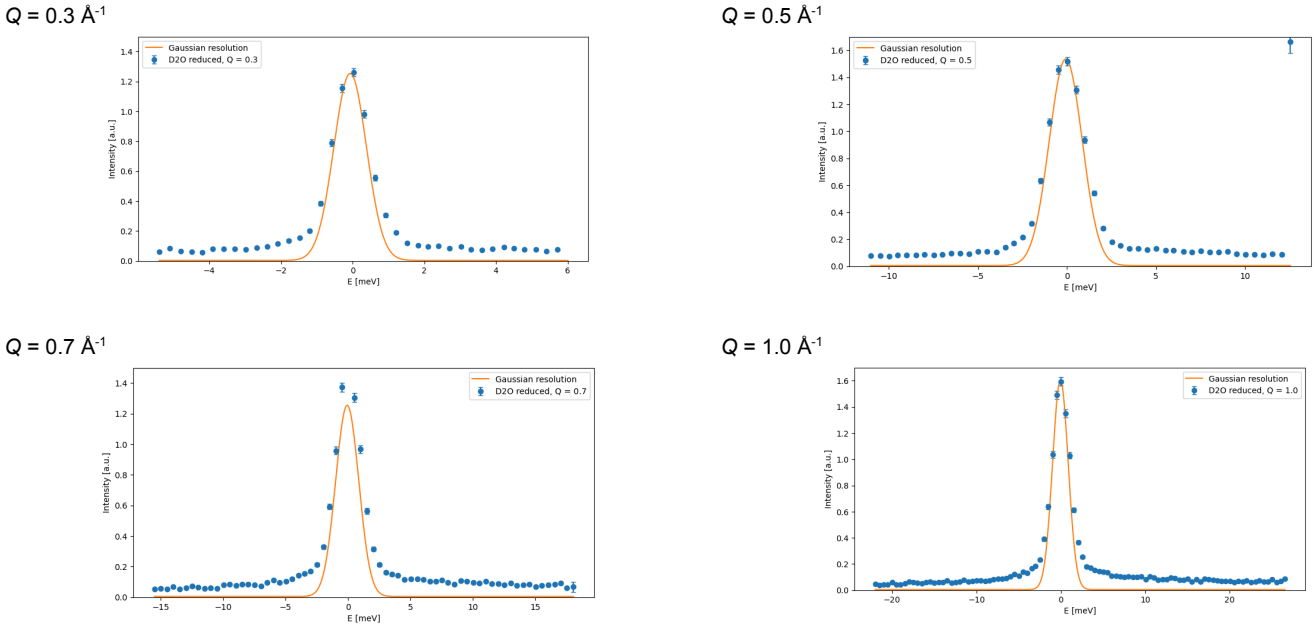

Figure 7. D_2O spectra at different *Q*-values. Background subtracted data are shown with blue dots, whereas the orange line is the experimental resolution (properly renormalized).

References

[1] A. Ivanov, private communication.

[2] A.J. Dianoux and G. Lander, *Neutron Data Booklet* (OCPG, 2003)